Natural Disaster Science, Volume 9, Number 1, 1987, pp. 99–113

RAPID ESTIMATION OF FAULT PARAMETERS FOR NEAR-FIELD TSUNAMI WARNING

Yasuo IZUTANI
Research Associate, Faculty of Engineering, Shinshu University
and
Tomowo HIRASAWA
Professor, Faculty of Science, Tohoku University

(Received 22 April, 1987 and in revised form 24 June, 1987)

ABSTRACT

A simple method is presented for rapid determination of fault parameters which are necessary to evaluate sea-bottom deformation due to large shallow earthquakes. Making use of the directivity of strong motion duration derived from observed accelerograms, we can estimate the fault length and the direction of rupture propagation. The values of the fault width and the slip amount are estimated from empirical formulae with respect to the fault length. The dip angle and the slip angle are assumed to be those of the typical focal mechanism in the focal region of the earthquake concerned. Our method is applied to the 1968 Tokachi-Oki earthquake and the 1983 Japan Sea earthquake. The estimated values of the fault parameters are consistent with those obtained previously by other investigators through the analyses of far-field long-period seismic waves, aftershock distribution, and so on. It is concluded that the present method is applicable to near-field tsunami warning, provided that a sufficient number of digital accelerographs are installed with a good azimuthal coverage.

1. INTRODUCTION

It is very important to issue tsunami warnings because the damage due to a tsunami caused by a large shallow earthquake occurring under the sea-bottom is often severer than that due to the earthquake ground motion. Tsunami warnings in Japan are issued by the Japan Meteorological Agency (JMA) within 17 minutes after an earthquake origin time [1]. These tsunami warnings are based on the hypocenter location and the maximum amplitudes of seismic records. The warning messages prepared by JMA are qualitative and classified into five types: 1) no tsunami, 2) tsunami alert, 3) tsunami, 4) major tsunami, and 5) cancellation.

Some efforts have been made toward developing quantitative tsunami warnings. Abe [2] deduced empirical relations among the maximum tsunami amplitude, the epicentral distance, and the magnitude scale M_t defined by Abe for tsunamigenic earthquakes. The M_t scale is essentially equivalent to the moment magnitude scale, which is the earthquake magnitude scale based on the seismic moment [3, 4]. Abe [2] concluded that his empirical formula would play an important role in predicting tsunami heights at observation sites if some method were available for quick determination of the seismic moment. Kanamori and Given [5] proposed the use of long-period seismic waves for rapid evaluation of the tsunami potential of earthquakes. They defined a measure of the tsunami potential by the product of the seismic moment and $\sin 2\delta$, where δ is the dip angle of the fault plane. The tsunami potential thus defined is of great use for near-field tsunami warnings, since it can rapidly be determined from the observed amplitudes of near-field long-period seismic waves. Okal and Talandier [6] found a relation between the

KEY WORDS: Tsunami warning, Fault parameters, Strong motion duration, Directivity
Note: Discussion open until 1 Sept., 1988

T-wave duration and the seismic moment, where the T-waves or T-phases are waves travelling through the ocean at the speed of sound in sea water. They proposed the use of the relation for real time estimation of the seismic moment.

All of these studies aimed at developing a method for the real time estimation of the maximum tsunami height or the tsunami potential. In the meantime, the recent remarkable progress in the capability of digital computers has been followed by great development of numerical techniques for simulating tsunami propagation [7]. Therefore, if we are able to determine the fault parameters necessary to compute sea-bottom deformation within a short time after an earthquake occurrence, it may be possible to issue quantitative tsunami warnings by estimating the arrival time and the height of a tsunami at an arbitrary coast.

The fault parameters necessary for computing sea-bottom deformation due to an earthquake are the following six: fault length, fault width, amount of slip, dip direction, dip angle, and slip angle. These parameters are currently evaluated based on the analysis of far-field long-period seismic waves and the spatial distribution of aftershocks. Since it is necessary to estimate the fault parameters within several minutes after an earthquake origin time, the aftershock distribution and far-field data cannot be used for the purpose of near-field tsunami warning.

Izutani and Hirasawa [8, 9] pointed out that the directivity effect due to the rupture propagation can be detected on the duration of strong ground motion derived from observed accelerograms. They developed a method for estimating the fault length and the direction of rupture propagation from the directivity. Since seismic records by digital accelerographs at observation stations with epicentral distances less than several hundred kilometers seem to be the most useful data immediately after an earthquake occurrence, the practical advantages of their method for near-field tsunami warnings should be obvious.

In the present study, combining the method by Izutani and Hirasawa [8, 9] with the empirical relations among the fault parameters by Abe [10] and the similarity in focal mechanisms of earthquakes occurring in the same region, we present a simple method for rapid determination of the fault parameters. The applicability of the present method will be tested through the estimation of the fault parameters for the Tokachi-Oki earthquake of May 16, 1968 and the Japan Sea earthquake of May 26, 1983.

2. METHOD

Figure 1 shows a flow chart of the present method for rapid estimation of the fault parameters of an earthquake. We assume that digital accelerograms and the information of the hypocenter location are obtainable immediately after the occurrence of a large shallow earthquake. Following this flow chart, we describe our method.

A Husid plot, $P(t)$, which is the cumulative power curve defined by

$$P(t)=\int_0^t \{x(t')*h(t')\}^2 dt' \Big/ \int_0^T \{x(t')*h(t')\}^2 dt', \tag{1}$$

is calculated from the observed accelerogram, where $x(t)$ is the ground acceleration, $h(t)$ is a band-pass filter between 5 and 10 Hz, and T is the total record length. The asterisk means the convolution. The band-pass filter is used to remove the contribution from surface waves. The strong motion duration (D) is obtained objectively as the time interval between $P(t)=0.05$ and $P(t)=0.85$. To cut $P(t)$ at 0.85 prevents D from being significantly affected by the total record length. Thus defined, the strong motion duration has no clear dependence on the source-to-site distance [11].

Examples of filtered ground acceleration and $P(t)$ are shown in Fig. 2. They are derived from north-south component accelerograms due to the Japan Sea earthquake of May 26, 1983. The strong motion duration (D) can be obtained by on-line data processing. It can be seen that the

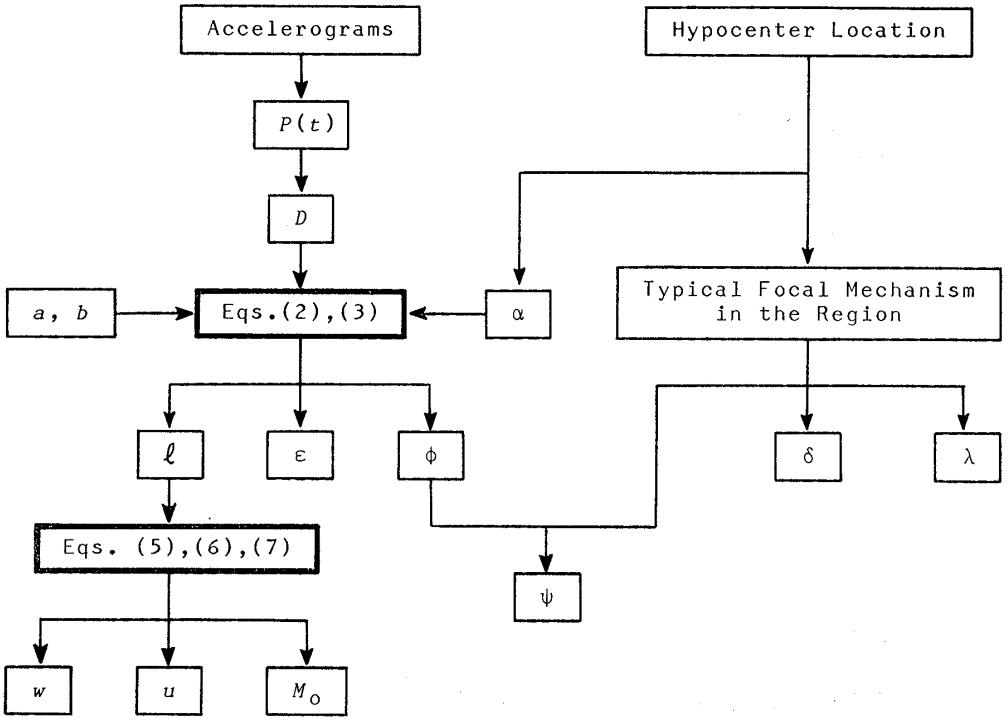

Fig. 1 Flow chart of the present method. $P(t)$, cumulative power curve of 5 to 10 Hz band-pass filtered ground acceleration; D, strong motion duration; a and b, site constants; α, station azimuth at the epicenter; l, total length of the fault; ε, ratio of the fault length of the shorter part to the total length; ϕ, direction of rupture propagation; ψ, dip direction; δ, dip angle; λ, slip angle; w, fault width; u, amount of slip; M_0, seismic moment.

strong motion durations at different observation stations, particularly Muroran-S and Akita-S, are very different from each other. This difference may be caused by the directivity due to the rupture propagation and also by the condition of surface layers at the observation stations.

According to Izutani and Hirasawa [9], the strong motion duration due to a large shallow earthquake is theoretically expected to be

$$D=(a/0.8)Fl+b, \tag{2}$$

where

$$\left.\begin{aligned} &F=\max\,[F^{\mathrm{L}}, F^{\mathrm{S}}],\\ &F^{\mathrm{L}}=(1-\varepsilon)\,\{(1-0.6\cos(\phi-\alpha)\},\\ &F^{\mathrm{S}}=\varepsilon\,\{1+0.6\cos(\phi-\alpha)\}. \end{aligned}\right\} \tag{3}$$

The top equation in Eq. (3) means that F is equal to the larger of F^L and F^S. The fault rupture is assumed to be propagated in the horizontal direction, that is, along the fault strike. This assumption is justified to a first approximation by the observational results [12, 13, 14, 15, 16] for large shallow earthquakes. Also, the ratio of the rupture velocity to the apparent velocity of S-waves is assumed to be 0.6. The constant of 0.6 in Eq. (3) results from these two assumptions. An asymmetric bilateral fault is considered here. The total fault length (l) is the sum of the length of the longer part, $(1-\varepsilon)l$, and that of the shorter part, εl, where $0\leqq\varepsilon\leqq0.5$. ϕ is the direction of rupture propagation on the longer part of the fault, and α is the azimuth of the observation station. Both ϕ and α are measured clockwise from the north at the earthquake epicenter. In order to take account of the local site effect at each observation station, a and b are introduced as site constants without regard to the earthquake source characteristics. They should be known

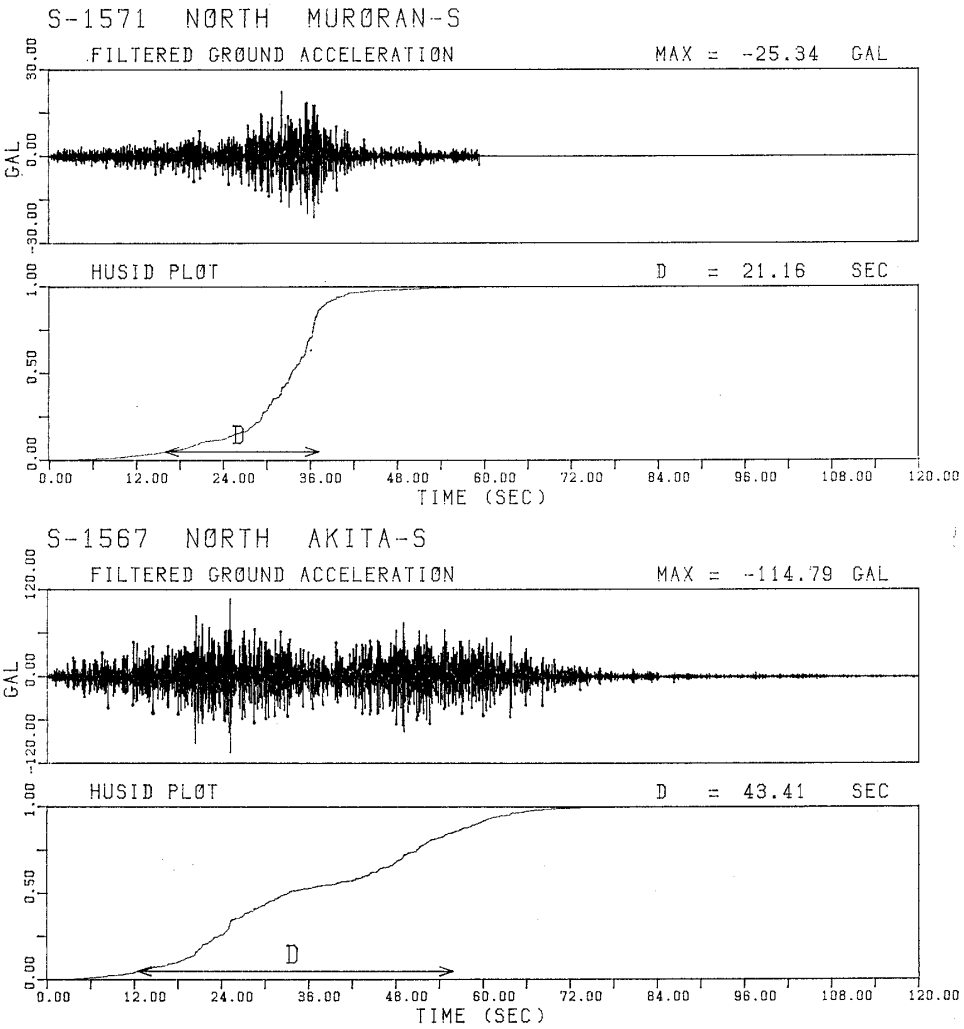

Fig. 2 Examples of 5 to 10 Hz band-pass filtered ground acceleration and Husid plot. D denotes the strong motion duration. Both examples are derived from north-south component accelerograms due to the 1983 Japan Sea earthquake.

quantities in estimating the fault parameters for near-field tsunami warnings. To determine them we simplify Eq. (2) by neglecting the directivity effect as

$$D=\hat{a}l+\hat{b}. \tag{4}$$

Average values of $\hat{a}$ and $\hat{b}$ for many past earthquakes are regarded as those of a and b at a given station. This procedure is inevitable in practice, because ε and ϕ are unknown for most past earthquakes. Furthermore, this procedure is statistically justified in the ideal case that $\varepsilon(0\leqq\varepsilon\leqq 0.5)$ and $\phi-\alpha(0\leqq\phi-\alpha<2\pi)$ are randomly and uniformly distributed in their domains. In this case the expectation of F in Eq. (3) with respect to ε and $\phi-\alpha$ becomes 0.8, which shows that the averages of $\hat{a}$ and $\hat{b}$ in Eq. (4) should be equivalent to a and b in Eq. (2).

Since the site constants are known for the stations concerned, the three source parameters of l, ε, and ϕ for an earthquake can be obtained by minimizing the sum of squares of residuals between the observed strong motion durations and the theoretical ones from Eqs. (2) and (3). We fix ε, in practice, at 0, 0.1, 0.2, 0.3, 0.4, or 0.5 to have a better convergence in the least squares procedure.

Abe [10] found that the fault length is about twice as long as the fault width, independent of the earthquake size, by analyzing the fault parameters of many large shallow earthquakes

which have occurred in and near Japan. He pointed out that the stress drop is 30 bars for earthquakes along the Japan trench and 60 bars for earthquakes inside the Japan arc. Making use of the dislocation model of earthquake source, he obtained empirical relationships between the fault parameters. Based on his results, we derive the following empirical formulae for the fault width (w), the amount of slip (u), and the seismic moment (M_0) with respect to the fault length (l):

$$w=l/2. \tag{5}$$

$$u=\begin{cases}2.17\ l & \text{(along the Japan Trench)}\\ 4.34\ l & \text{(inside the Japan Arc).}\end{cases} \tag{6}$$

$$M_0=\begin{cases}4.35\times10^{21}\ l^3 & \text{(along the Japan Trench)}\\ 8.70\times10^{21}\ l^3 & \text{(inside the Japan Arc).}\end{cases} \tag{7}$$

The rigidity of the materials in the focal region is assumed to be 4×10^{11} dyne/cm^2 in the present study. l and w are in km, u in cm, and M_0 in dyne·cm.

It is known that the focal mechanisms are all nearly the same for large shallow earthquakes in a given tectonic region [5, 17]. Therefore, it is possible to predict with reasonable accuracy the dip angle (δ) and slip angle (λ) of an earthquake from the typical focal mechanism of past earthquakes in the same tectonic region. As mentioned before, the direction of rupture propagation (ϕ) is considered to be nearly equal to the direction of the fault strike. Accordingly, the dip direction (ψ), which is nearly equal to $\phi+90°$ or $\phi-90°$, can be found from the least squares procedure for the source parameters of l, ε, and ϕ.

3. APPLICATION

3.1. *Tokachi-Oki Earthquake of May* 16, 1968

Accelerograms observed at five stations, as listed in Table 1, are available for the Tokachi-Oki earthquake. Before going into the problem of source parameter determination, we have to estimate the site constants at the five stations. Figure 3 shows the strong motion durations obtained at these stations for past earthquakes whose focal depths range from 0 to 60 km. They are plotted against the fault length l. We use the values of l which have been determined by previous studies through the analyses of aftershock distribution, far-field long-period seismic waves, and so on. For earthquakes whose fault lengths have not been presented, l is estimated

Table 1 Data for the Tokachi-Oki earthquake.

Station*	D (sec)	α (degree)	a (sec/km)	b (sec)	W	l_{max} (km)
Kushiro-S	33.14	14.50	0.189	5.75	1.0	180
Muroran-S	21.41	309.72	0.162	4.62	0.5	100
Aomori-S	24.79	273.24	0.234	5.69	0.5	100
Hachinohe-S	52.00	264.16	0.300	5.98	0.5	100
Miyako-S	66.34	228.94	0.182	5.40	0.5	90

* The capital letter at the end of a station name distinguishes the type of the accelerograph operated at the station by the Port and Harbour Research Institute of the Ministry of Transport, Japan. The letter *S* means SMAC-B2 accelerograph, and the letter M, which will appear in Table 4, ERS accelerograph.
D, observed strong motion duration for the Tokachi-Oki earthquake;
α, station azimuth at the epicenter;
a and b, site constants obtained from data excluding the Tokachi-Oki earthquake;
W, weight;
l_{max}, the largest value of the fault length among the data used to obtain a and b.

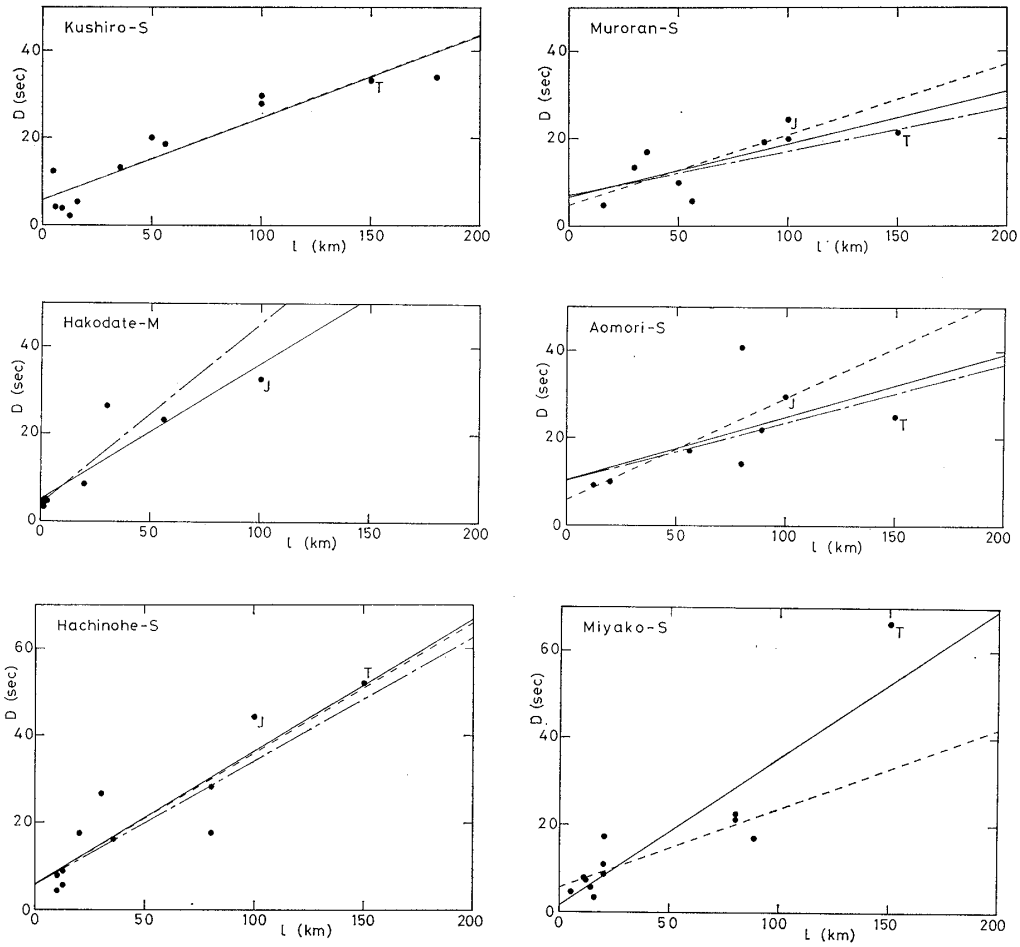

Fig. 3 Strong motion duration (D) plotted against the fault length (l). Data marked with a **T** or **J** are due to the 1968 Tokachi-Oki earthquake or the 1983 Japan Sea earthquake. The lines indicate the least squares fit for the data. The solid line, for all the data; the dashed line, for the data set excluding the data marked **T**; the chained line, for the data set excluding the data marked **J**.

from the earthquake magnitude using the empirical formula of Otsuka [18]. Based on Eq. (4), the site constants (a, b) listed in Table 1 are obtained from the dashed lines in Fig. 3, which are least squares fits for the data set without the data of the Tokachi-Oki earthquake. The reason why we exclude the data is simply because we are to determine the fault parameters of the Tokachi-Oki earthquake.

The strong motion durations D in Table 1 are average values of those obtained independently from two horizontal components of accelerograms observed for the Tokachi-Oki earthquake at the five stations. The azimuthal coverage of these stations is about 150 degrees around the epicenter. The site constants of the Kushiro-S station were determined from data distributed over a wider range of fault lengths than those of the other stations, as seen in Fig. 3. In the source parameter determination, therefore, we give a smaller weight, say 0.5, to the other four stations, as listed in Table 1.

The source parameters obtained from the least squares analysis based on Eqs. (2) and (3) are listed in Table 2. The standard deviations of Solutions 1 to 3 are the same and smaller than those of the other solutions. To have an easier comparison between observation and theory, let us define the apparent fault length L by

$$L=0.8\ (D-b)/a. \tag{8-a}$$

This is rewritten from Eq. (2) by

$$L=Fl. \tag{8-b}$$

The observed values of apparent fault length L are calculated from Eq. (8-a) and the data in Table 1, and plotted against the azimuth of station in Fig. 4. The theoretical function L of azimuth expressed by Eq. (8-b) is the same for Solutions 1 to 3 and shown by the solid curve in Fig. 4.

It may easily be understood from Eq. (3) that F^L is always larger than F^S, irrespective of the azimuth, when ε is smaller than 0.2. In such cases, the length of the longer part of the fault, $(1-\varepsilon)l$, takes a definite value without regard to the value of ε, but the length of the shorter part,

Table 2 Least squares solution for the Tokachi-Oki earthquake.

Solution No.	ε	l (km)	ϕ (degree)	σ (sec)
1	0.0*	192±33	322±14	8.99
2	0.1*	213±37	322±14	8.99
3	0.2*	240±41	322±14	8.99
4	0.3*	261±64	324±23	9.71
5	0.4*	206±63	355±38	11.45
6	0.5*	179±46	30±49	13.69

* Assumed value.
ε, ratio of the fault length of the shorter part to the total length;
l, total length of the fault;
ϕ, direction of the rupture propagation;
σ, standard deviation.

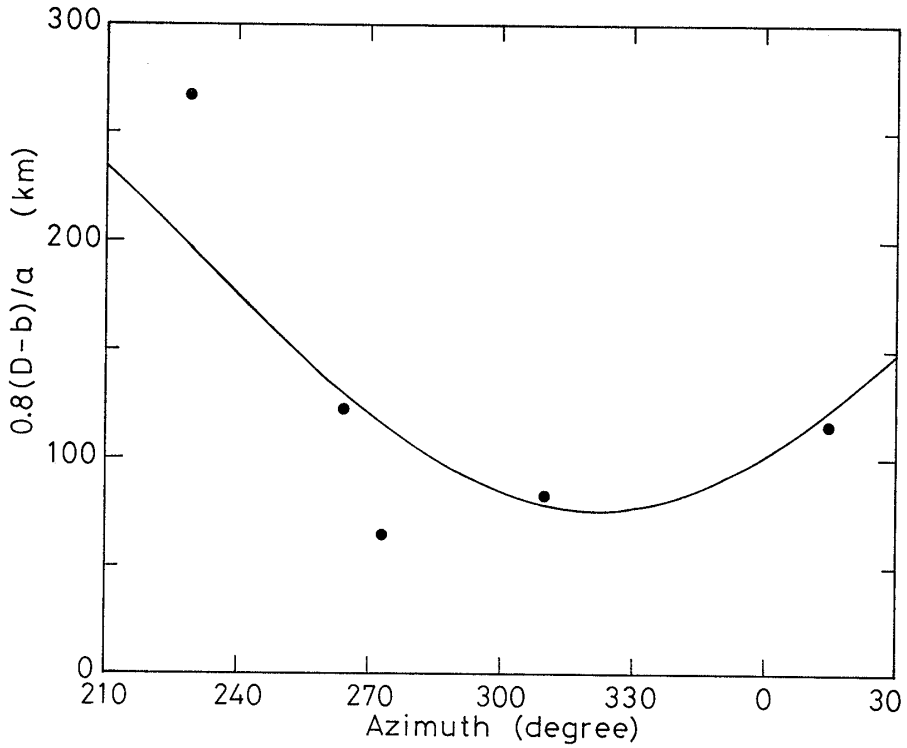

Fig. 4 Apparent fault length (L) plotted against the station azimuth for the 1968 Tokachi-Oki earthquake. The solid circles indicate observations, and the solid curve indicates the theoretical function L expected for Solutions 1 to 3 in Table 2.

εl, is indefinite. Since we want to know the fault length for the purpose of tsunami warnings, we should adopt Solution 3 to avoid underestimation of the fault length.

The lengths and the directions of the arrows in Fig. 5 indicate the fault length and the direction of rupture propagation in Solution 3. The starting point of the asymmetric bilateral rupture is placed at the hypocenter. The fault model by Kanamori [14], which was derived from far-field data, and the approximate aftershock area are also shown in Fig. 5. The rupture process of the Tokachi-Oki earthquake has been studied in detail not only by Kanamori [14] but also by many other investigators [19, 20, 21, 22, 23, 24, 25]. According to these studies, the rupture process is characterized by predominantly unilateral rupture propagation in the direction of N to NW over a length of 150 to 200 km. The present results for rupture propagation on the longer part of the fault are satisfactorily consistent with the results of these previous studies.

The fault width, the amount of slip, and the seismic moment are estimated by means of Eqs. (5), (6), and (7) for Solutions 1 and 3, as listed in Table 3. The focal mechanism is assumed to be a thrust fault dipping by 20° toward the west, based on the tectonic features of the northern part of the Sanriku-Oki region [17]. The dip direction is obtained from ϕ as $-128°$. The slip angle is calculated by making use of the average motion direction of the foot-wall block against

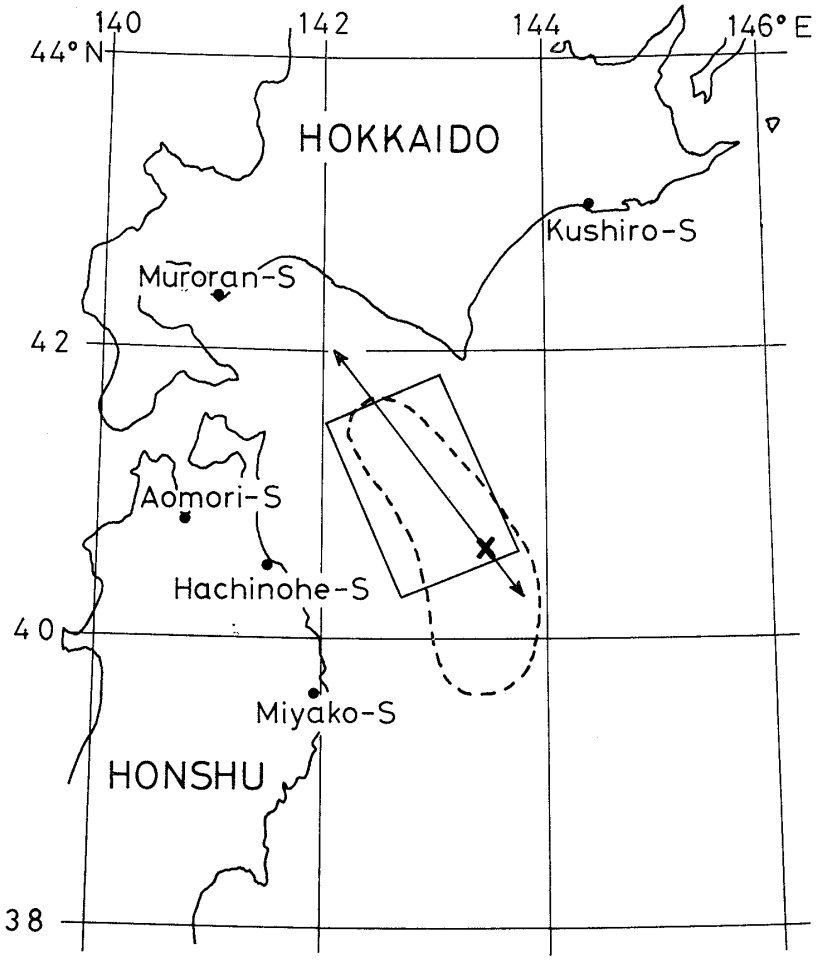

Fig. 5 The fault length and the direction of rupture propagation for the 1968 Tokachi-Oki earthquake. The cross and the dashed curve denote the epicenter of the main shock and the approximate epicentral area of the aftershocks. The rectangle indicates the fault model by Kanamori [14]. The present result (Solution 3 in Table 2) is illustrated by the arrows whose length and direction show the fault length and direction of rupture propagation.

Table 3 Fault parameters of the Tokachi-Oki earthquake.

	l (km)	w (km)	ψ (°)	δ (°)	λ (°)	u (m)	M_0 ($\times 10^{28}$ dyne·cm)
Present Study*	192	96	−128	20	152	4.2	3.1
Present Study#	240	120	−128	20	152	5.2	6.0
Kanamori [14]	150	100	−114	20	142	4.1	2.8

* Based on Solution 1 ($\varepsilon=0$) in Table 2.
\# Based on Solution 3 ($\varepsilon=0.2$) in Table 2.
l, length; w, width; ψ, dip direction; δ, dip angle; λ, slip angle; u, amount of slip; M_0, seismic moment.

the hanging-wall side, that is, N65°W for earthquakes in the region [17]. In Table 3, the fault parameters by Kanamori [14] are also listed for comparison. As stated before, the fault length of Solution 3 should be regarded as an upper bound. The overestimation of the fault length results in overestimations for the fault width, the amount of slip, and the seismic moment, as compared with the result by Kanamori [14]. However, the present result based on Solution 1 agrees well with the result by Kanamori [14].

3.2. *Japan Sea Earthquake of May* 26, 1983

The horizontal component accelerograms to be analyzed for the 1983 Japan Sea earthquake were observed at the nine stations listed in Table 4. The azimuthal coverage of these stations is about 130° around the epicenter. The site constants (a, b) for four stations (Muroran-S, Hakodate-M, Aomori-S, Hachinohe-S) are estimated from the chained lines in Fig. 3 and shown in Table 4. The value of 0.5 is given to the weight for Hakodate-M for the same reason as for the Tokachi-Oki earthquake.

The site constants cannot be obtained for the other five stations because the number of data from past earthquakes is too small. The relations (the solid lines in Fig. 3) between the strong motion duration and the fault length are gathered together in Fig. 6. Since the relation for Kushiro-S shows an average tendency, we tentatively assume that the site constants of the five

Table 4 Data for the Japan Sea earthquake.

Station	D (sec)	α (degree)	a (sec/km)	b (sec)	W	l_{max} (km)
Muroran-S	24.33	35.45	0.108	6.81	1.0	150
Hakodate-M	32.59	40.83	0.412	4.01	0.5	60
Shiranuka	33.29	51.32	0.187*	5.81*	0.25	—
Furofushi	31.16	66.96	0.187*	5.81*	0.25	—
Aomori-S	29.34	70.30	0.134	10.33	1.0	150
Hirosaki	34.65	77.49	0.187*	5.81*	0.25	—
Hachinohe-S	44.26	83.24	0.281	6.08	1.0	150
Akita-S	43.53	125.91	0.187*	5.81*	0.25	—
Sakata-S	47.02	157.79	0.187*	5.81*	0.25	—

* Assumed value.
D, observed strong motion duration for the Japan Sea earthquake;
α, station azimuth at the epicenter;
a and b, site constants obtained from data excluding the Japan Sea earthquake;
W, weight;
l_{max}, the largest value of the fault length among the data used to obtain a and b.

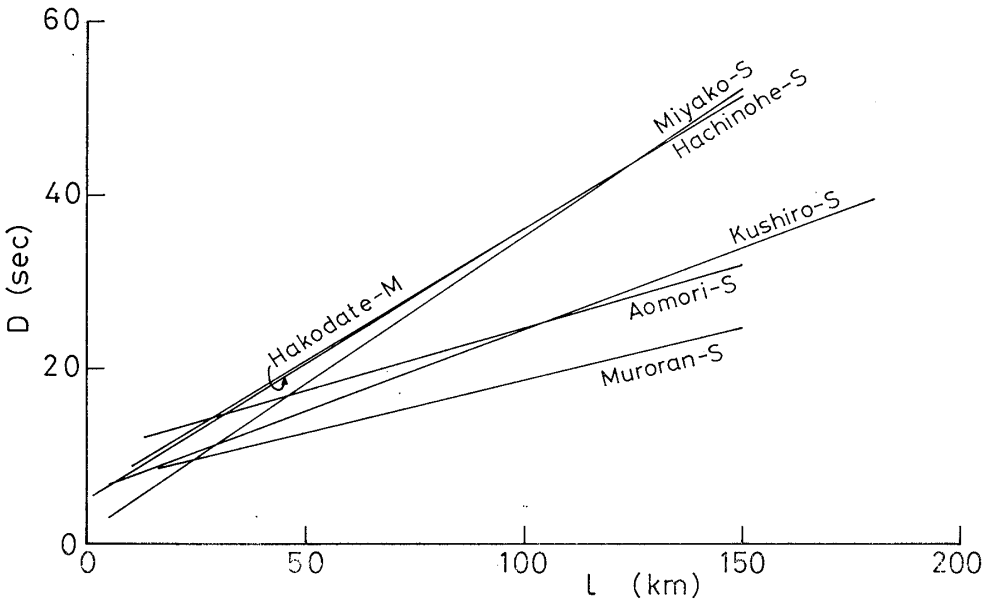

Fig. 6 Relations between the strong motion duration (D) and the fault length (l).

stations have the same values as those of Kushiro-S. Taking into account this uncertainty for the site constants, the weights are taken to be 0.25 for these stations, as shown in Table 4.

Shimazaki and Mori [26] studied the source process of the Japan Sea earthquake by analyzing far-field long-period seismic waves, and found that the earthquake consisted of two major events. The rupture paused for about 10 seconds between the two events. In order to take account of the effect of the pause in rupture propagation, we introduce one more unknown parameter (τ) into Eq. (2) as

$$D=(a/0.8)Fl+b+\tau, \tag{9}$$

where the expression for F is the same as that in Eq. (3).

Solutions for only three cases ($\varepsilon=0$, 0.1, 0.2) were obtained by the least squares method, as shown in Table 5. For the other cases ($\varepsilon=0.3$, 0.4, 0.5), we found different solutions from different assumptions of the initial values. Furthermore, the standard deviations of these solutions are larger than those in the cases of $\varepsilon\leqq 0.2$. Therefore, the results in the cases of $\varepsilon\geqq 0.3$ are omitted in Table 5. As in the case of the Tokachi-Oki earthquake, the lengths of the longer part of the fault are the same, 85 km, for Solutions 1 to 3. On the other hand, the fault length of the

Table 5 Least squares solution for the Japan Sea earthquake.

Solution No.	ε	l (km)	ϕ (degree)	τ (sec)	σ (sec)
1	0.0*	85±16	7±19	11±2	2.12
2	0.1*	94±18	7±19	11±2	2.12
3	0.2*	106±21	7±19	11±2	2.12

* Assumed value.
ε, ratio of the fault length of the shorter part to the total length;
l, total length of the fault;
ϕ, direction of the rupture propagation;
τ, pause interval of the fault rupture;
σ, standard deviation.

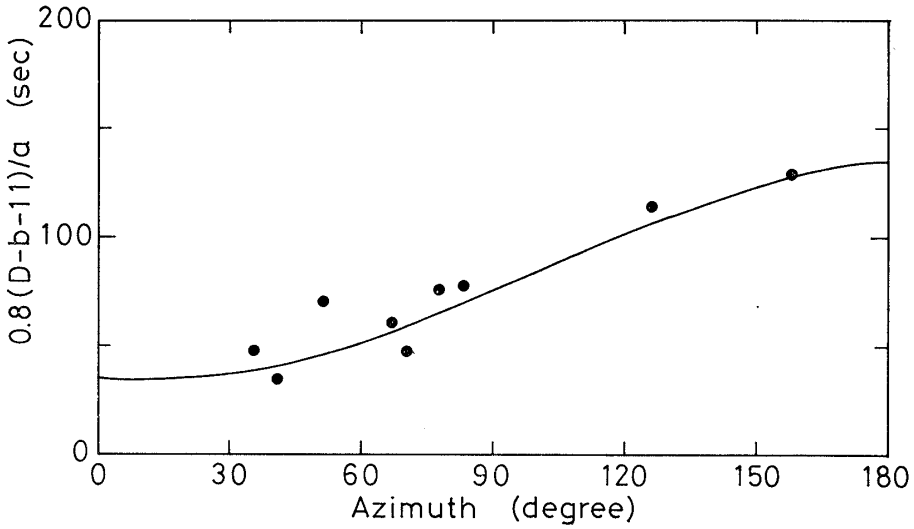

Fig. 7 Apparent fault length (L) plotted against the station azimuth for the 1983 Japan Sea earthquake. The solid circles indicate observations, and the solid curve indicates the theoretical function L expected for Solutions 1 to 3 in Table 5.

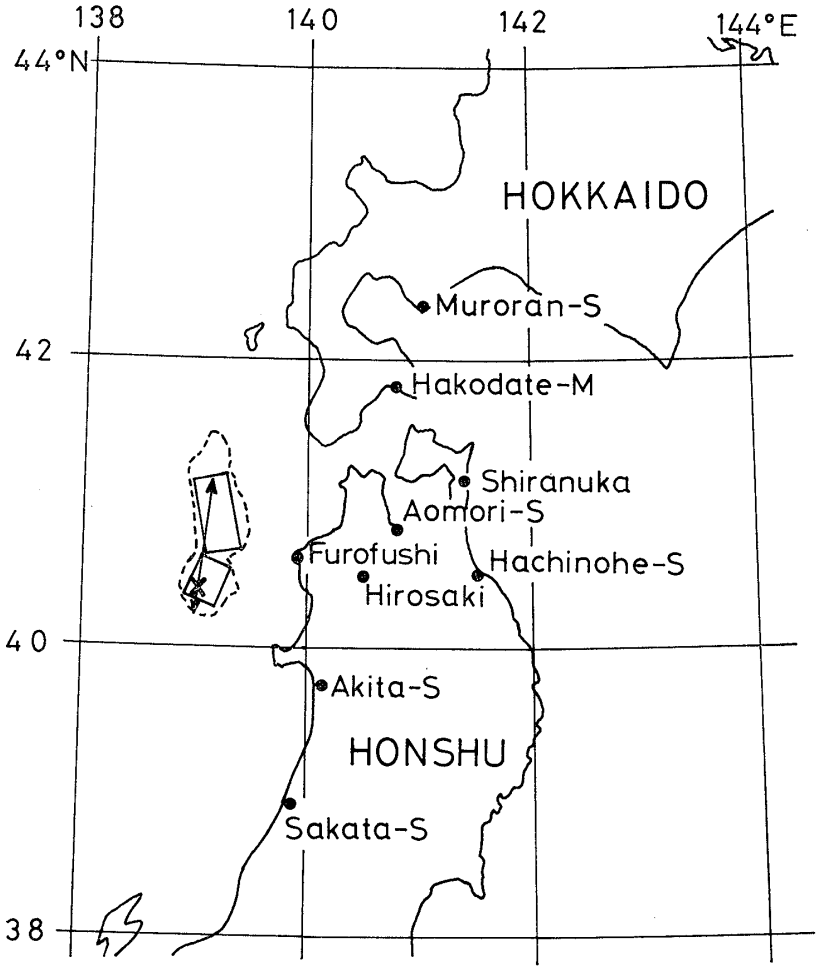

Fig. 8 The fault length and the direction of rupture propagation for the 1983 Japan Sea earthquake. The cross and the dashed curve denote the epicenter of the main shock and the approximate epicentral area of aftershocks. The rectangles indicate the fault model by Shimazaki and Mori [26]. The present result (Solution 3 in Table 5) is illustrated by the arrows whose length and direction show the fault length and direction of rupture propagation.

Table 6 Fault parameters of the Japan Sea earthquake.

		l (km)	w (km)	ϕ (°)	δ (°)	λ (°)	u (m)	M_0 ($\times 10^{27}$ dyne·cm)
Present Study*		85	42	97	30	90	3.7	5.3
Present Study#		106	53	97	30	90	4.6	10.4
Shimazaki and Mori [26]	(N)	60	40	90	25	90	4	5.1~5.8
	(S)	35	30	90	25	90	6	
Kosuga et al. [29]	(N)	60	40	80	20	90	4	2.9
	(S)	30	35	105	20	90	6	1.9
Satake [30]	(N)	60	40	70	30	90	4	7.56
	(S)	60	40	110	30	90	5	

* Based on Solution 1 ($\varepsilon=0$) in Table 5.
\# Based on Solution 3 ($\varepsilon=0.2$) in Table 5.
(N), northern part of the fault; (S), southern part of the fault.
l, length; w, width; ϕ, dip direction; δ, dip angle; λ, slip angle; u, amount of slip; M_0, seismic moment.

shorter part is indefinite and in a range between 0 and 21 km.

Similarly to Eqs. (8-a, b), we define the apparent fault length by

$$L=0.8\ (D-b-11)/a, \tag{10-a}$$

and rewrite this as

$$L=Fl. \tag{10-b}$$

The observed data calculated from Eq. (10-a) are plotted against the station azimuth in Fig. 7. The solid curve in the figure is the theoretical one by Eq. (10-b), and well accounts for the observations. The fault length and the direction of rupture propagation in Solution 3 are shown by the arrows in Fig. 8. It may be seen that our result is consistent with that by Shimazaki and Mori [26] as well as the aftershock area. It is noted that the pause interval of rupture propagation is estimated at 11 seconds. This agrees very well with the value of about 10 seconds obtained by Shimazaki and Mori [26] and Sato [27].

The fault parameters based on Solutions 1 and 3 are given in Table 6, where the focal mechanism of the Niigata earthquake of June 16, 1964 [28] is regarded as a typical one in the tectonic region under consideration. The focal mechanism of the present earthquake is thus assumed to be a thrust fault dipping by 30° toward the east. For the sake of comparison, we give in Table 6 the results obtained by other investigators [26, 29, 30] from long-period far-field seismic data, tsunami data, aftershock distribution, and geodetic data. From this the present result based on Solution 1 ($\varepsilon=0$) is found to underestimate slightly the fault length and the amount of slip, while the result based on Solution 3 ($\varepsilon=0.2$) somewhat overestimates the fault width and the seismic moment.

4. DISCUSSION AND CONCLUSION

Since estimation of fault parameters by the present method depends significantly on the estimated values of the site constants (a, b), it is very important to determine accurately the site constants for each observation station by analyzing strong motion data from as many past earthquakes as possible. Unfortunately, however, the available strong motion data are not sufficient either in quality or in quantity to obtain reliable estimates of a and b for many stations. Especially, the scantiness of data from large earthquakes is unavoidable in usual cases. The extrapolation of the relation between the strong motion duration and the fault length may lead to unstable esti-

mates for the site constants. Therefore, the site constants should be improved whenever new data, from large earthquakes in particular, are obtained.

The azimuthal coverage by observation stations around the epicenter is also an important factor in obtaining reliable and stable least squares solutions. Observation stations are generally on land, while large earthquakes generating tsunami take place beneath the sea. The azimuthal coverage around the epicenter by the observation stations now available in Japan is 150 degrees at most. If it becomes possible to make use of data from some ocean-bottom accelerograph stations, we will be able to obtain more reliable and stable least squares solutions.

The uncertainty of the fault length when $\varepsilon \leqq 0.2$ is an inevitable limitation of the present method. One positive way to overcome this limitation is the use of some amplitude information of strong ground motion in addition to the strong motion duration. It may be necessary, however, to develop a more complicated method than the present one, and the on-line data processing may become difficult. In the present study, we discussed the two extreme solutions, that is, Solution 1 for $\varepsilon=0$ and Solution 3 for $\varepsilon=0.2$. This uncertainty for the fault length causes a difference in seismic moment by a factor of about 2. Nevertheless, the fault parameters by various investigators are satisfactorily consistent with those based either on Solution 1 or on Solution 3, as shown before. In other words, the difference in fault parameters between our two extreme cases does not significantly exceed the amount of scatter in those estimated by other investigators. This suggests the practical usefulness of our simple method. For the purpose of tsunami warnings, we have proposed in the present paper to adopt Solution 3 for $\varepsilon=0.2$ in order to avoid possible underestimations for tsunami heights. However, if independent information is available for the seismic moment, by such a method as that proposed by Kanamori and Given [5], for example, the estimation of tsunami height should be more reliable.

It is remarked that the earthquakes adopted for the applied examples of our method in this study are not tsunami earthquakes but normal earthquakes. The tsunami earthquake is defined as an earthquake generating an anomalously large tsunami compared with that expected for its earthquake magnitude. As is well known, its typical example is the 1896 Sanriku-Oki earthquake. Among recent earthquakes, the Hokkaido Toho-Oki earthquake of June 10, 1975, with JMA magnitude 7.0 can be classified into the tsunami earthquake. Its tsunami magnitude is 1.5 according to Hatori [31]. Unfortunately, we could not adopt this earthquake as an applied example of our method, simply because no observed accelerograms with satisfactory S/N ratios were available. It is generally considered that the tsunami earthquake is not so efficient in generating high-frequency seismic waves. However, our method is based on the observed strong motion durations. As may be understood from its definition, the strong motion duration can properly be determined from an observed accelerogram even in the case where its maximum amplitude is small. We think, therefore, that our method is effective even for tsunami earthquakes, provided that accelerograms with a sufficiently good S/N ratio are available from the strong motion observation with a high sensitivity.

We conclude that our simple method can rapidly give reasonable estimates of the fault parameters for a large shallow earthquake. This method may thus be applicable to near-field tsunami warnings that quantitatively forecast the arrival times and the heights of tsunamis within a short time after earthquake occurrences.

ACKNOWLEDGEMENTS

The digital data of accelerograms analyzed in this study were supplied by the Port and Harbour Research Institute, the Central Research Institute of the Electric Power Industry, and by Hirosaki University. We thank the members concerned of these research institutes. We also thank Prof. N. Shuto of the Faculty of Engineering, Tohoku University, for his invaluable suggestions. This study was supported partly by a Grant-in-Aid for Research on Natural Disasters from the

Ministry of Education, Science and Culture, Japan. Calculations were made at the Computer Centers of Shinshu University and the University of Tokyo. Least squares solutions were obtained using the "Program System SALS" [32].

REFERENCES

[1] Ichikawa, M. and Watanabe, H. (1983). A new system for tsunami warning in the Japan Meteorological Agency, in Tsunamis—Their Science and Engineering, ed. K. Iida and T. Iwasaki, Terra Scientific Pub. Co., Tokyo, pp. 51–60.

[2] Abe, K. (1981). Physical size of tsunamigenic earthquakes of the northwestern Pacific, Phys. Earth Planet. Inter., Vol. 27, pp. 194–205.

[3] Abe, K. (1979). Size of great earthquakes of 1837–1974 inferred from tsunami data, J. Geophys. Res., Vol. 84, pp. 1561–1568.

[4] Kanamori, H. (1977). The energy release in great earthquakes, J. Geophys. Res., Vol. 82, pp. 2981–2987.

[5] Kanamori, H. and Given, J.W. (1983). Use of long-period seismic waves for rapid evaluation of tsunami potential of large earthquakes, in Tsunamis—Their Science and Engineering, ed. K. Iida and T. Iwasaki, Terra Scientific Pub. Co., Tokyo, pp. 37–49.

[6] Okal, E.A. and Talandier, J. (1986). T-wave duration, magnitudes and seismic moment of an earthquake—Application to tsunami warning, J. Phys. Earth, Vol. 34, pp. 19–42.

[7] Goto, C. and Shuto, N. (1985). Accuracy and speed of numerical simulation as a means of tsunami forecasting, Proc. Intern. Tsunami Symp., pp. 82–87.

[8] Izutani, Y. and Hirasawa, T. (1984). Strong motion durations and source parameters, Prog. Abstr. Seismol. Soc. Japan, No. 1, p. 197 (in Japanese).

[9] Izutani, Y. and Hirasawa, T. (1987). Use of strong motion duration for rapid evaluation of fault parameters, J. Phys. Earth, Vol. 35, pp. 171–190.

[10] Abe, K. (1975). Reliable estimation of the seismic moment of large earthquakes, J. Phys. Earth, Vol. 23, pp. 381–390.

[11] Izutani, Y. (1983). Analysis of accelerograms and prediction of strong ground motion based on a stochastic source model, Ph. D. thesis, Tohoku Univ. Sendai.

[12] Kanamori, H. (1970). Synthesis of long-period surface waves and its application to earthquake source studies—Kurile Island earthquake of October 13, 1963, J. Geophys. Res., Vol. 75, pp. 5011–5027.

[13] Kanamori, H. (1970). The Alaska earthquake of 1964: Radiation of long-period surface waves and source mechanism, J. Geophys. Res., Vol. 75, pp. 5029–5040.

[14] Kanamori, H. (1971). Focal mechanism of the Tokachi-Oki earthquake of May 16, 1968: Contortion of the lithosphere at a junction of two trenches, Tectonophysics, Vol. 12, pp. 1–13.

[15] Abe, K. (1973). Tsunami and mechanism of great earthquakes, Phys. Earth Planet. Inter., Vol. 7, pp. 143–153.

[16] Kanamori, H. and Cipar, J.J. (1974). Focal process of the great Chilean earthquake of May 22, 1960, Phys. Earth Planet. Inter., Vol. 9, pp. 128–136.

[17] Izutani, Y. and Hirasawa, T. (1978). Source characteristics of shallow earthquakes in the northern part of Sanriku-Oki region, Japan, J. Phys. Earth, Vol. 26, pp. 275–297.

[18] Otsuka, M. (1964). Earthquake magnitude and surface fault formation, J. Phys. Earth, Vol. 12, pp. 19–24.

[19] Nagamune, T. (1971). Source regions of great earthquakes, Geophys. Mag., Vol. 35, pp. 333–399.

[20] Fukao, Y. and Furumoto, M. (1975). Foreshocks and multiple shocks of large earthquakes, Phys. Earth Planet. Inter., Vol. 10, pp. 355–368.

[21] Iida, M. and Hakuno, M. (1984). The difference in the complexities between the 1978 Miyagi-Oki earthquake and the 1968 Tokachi-Oki earthquake from a viewpoint of the short-period range, Natural Disaster Sci., Vol. 6, No. 2, pp. 1–26.

[22] Mori, J. and Shimazaki, K. (1984). High stress drops of short-period subevents from the 1968 Tokachi-Oki earthquake as observed on strong motion records, Bull. Seismol. Soc. Am., Vol. 74, pp. 1529–1544.

[23] Mori, J. and Shimazaki, K. (1985). Inversion of intermediate-period Rayleigh waves for source

characteristics of the 1968 Tokachi-Oki earthquake, J. Geophys. Res., Vol. 90, pp. 11374–11382.
[24] Kikuchi, M. and Fukao, Y. (1985). Iterative deconvolution of complex body waves from great earthquakes—the Tokachi-Oki earthquake of 1968, Phys. Earth Planet. Inter., Vol. 37, pp. 235–248.
[25] Schwartz, S.Y. and Ruff, L. (1985). The 1968 Tokachi-Oki and the 1969 Kurile Islands earthquakes: Variability in the rupture process, J. Geophys. Res., Vol. 90, pp. 8613–8626.
[26] Shimazaki, K. and Mori, J. (1983). Focal mechanism of the May 26, 1983 Japan Sea earthquake, Prog. Abstr. Seismol. Soc. Japan, No. 2, p. 15.
[27] Sato, T. (1985). Rupture characteristics of the 1983 Nihonkai-Chubu (Japan Sea) earthquake as inferred from strong motion accelerograms, J. Phys. Earth, Vol. 33, pp. 525–557.
[28] Hirasawa, T. (1965). Source mechanism of the Niigata earthquake of June 16, 1964, as derived from body waves, J. Phys. Earth, Vol. 13, pp. 35–66.
[29] Kosuga, M., Sato, T., Tanaka, K. and Sato, H. (1984). Aftershock activities and fault model of the Japan Sea earthquake of 1983, Sci. Rep. Hirosaki Univ., Vol. 31, pp. 55–69 (in Japanese).
[30] Satake, K. (1985). The mechanism of the 1983 Japan Sea earthquake as inferred from long-period surface waves and tsunamis, Phys. Earth Planet. Inter., Vol. 37, pp. 249–260.
[31] Hatori, T. (1978). Tsunami magnitude and seismic moment, Zisin, Ser. 2, Vol. 31, pp. 25–34 (in Japanese).
[32] Nakagawa, T. and Oyanagi, Y. (1980). Program system SALS for nonlinear least-squares fitting in experimental sciences, in Recent Developments in Statistical Inference and Data Analysis, ed. K. Matsushita, North Holland Pub. Co., Amsterdam, pp. 221–225.